

Polyakov loop distributions near deconfinement in $SU(2)$ lattice gauge theory[★]

J. Engels, J. Fingberg, M. Weber

Fakultät für Physik, Universität Bielefeld, D-4800 Bielefeld, Federal Republic of Germany

Received 6 July 1988

Abstract. The distribution function of the Polyakov loop is investigated on a $16^3 \times 3$ lattice in the neighbourhood of the deconfinement transition of $SU(2)$ gauge theory. We find, that well above the transition the distribution is a Gaussian; when the coupling approaches the critical point it is modified due to phase flip attempts of the system. Corresponding distributions for the plaquettes remain, however, Gaussian. For one coupling close to the transition we study the distributions on 8^3 , 12^3 and $18^3 \times 4$ lattices and show that strong finite size effects are present. Using the maximum values of the Gaussian parts of the distributions we construct a more physical (and therefore scaling) order parameter whose critical exponent is in excellent agreement with the universality hypothesis.

1 Introduction

The investigation of the deconfinement transition of $SU(2)$ gauge theory at finite temperature is seriously hampered by the fact that all numerical evaluations of the theory have to be carried out on finite lattices. The expectation value $\langle L \rangle$ of the Polyakov loop (thermal Wilson line) is the order parameter for the deconfinement transition on an infinite lattice. It is zero in the confinement region, i.e. below a critical coupling or critical temperature T_c , whereas in the deconfinement regime two (for $SU(2)$) equivalent states exist, for which $\langle L \rangle$ is finite and which differ in the sign of $\langle L \rangle$. Since on a finite lattice there is always a finite probability for tunneling between the two states, the measured value for $\langle L \rangle$ has to approach zero everywhere with increasing statistics. The way out of this dilemma is usually to take the expectation value of the modulus of the lattice average, $\langle \bar{L} \rangle$, as order parameter. Due to the non-zero fluctuation of L -values

on finite lattices, however, the quantity $\langle \bar{L} \rangle$ never becomes zero and therefore cannot act as a true order parameter. The interesting parameters characterizing the second order deconfinement transition in $SU(2)$, i.e. the critical temperature and the critical exponents can then only approximately be determined on a finite lattice and the results depend not only on the size of the lattice but also on the prescriptions to obtain them.

Before we review the presently known facts let us introduce our notation. The Polyakov loop for $SU(2)$ gauge theory on an $N_\sigma^3 \times N_\tau$ lattice is defined as

$$L(\mathbf{x}) = \frac{1}{2} \text{Tr} \prod_{r=1}^{N_\tau} U_{r,\mathbf{x};0}, \quad (1)$$

where $U_{x;0}$ are the $SU(2)$ link matrices at four-position x in time direction. We use the standard Wilson action [1]

$$S(U) = \frac{4}{g^2} \sum_P \text{Tr} U_P; \quad (2)$$

here U_P is the product of link operators around a plaquette. Let us denote the lattice average of $L(\mathbf{x})$ by L without index, then

$$\bar{L} = |L| = \left| \frac{1}{N_\sigma^3} \sum_{\mathbf{x}} L(\mathbf{x}) \right|. \quad (3)$$

As is well-known [2] the order parameter measures the free energy F_q of a single static (infinite mass) quark at temperature T

$$\langle L \rangle \sim \exp\left(-\frac{F_q}{T}\right), \quad (4)$$

where T is connected to the lattice spacing a by

$$T = \frac{1}{N_\tau a}. \quad (5)$$

Usually the temperature for a given coupling constant g^2 is obtained from (5) by assuming the asymptotic

[★] Work supported by the Deutsche Forschungsgemeinschaft, under research grant En 164/2

scaling relation for $a(g^2)$

$$a(g^2)\Lambda_L = \exp \left\{ -\frac{12\pi^2}{11g^2} + \frac{51}{121} \ln \left(\frac{24\pi^2}{11g^2} \right) \right\}. \quad (6)$$

However, the last equation only approximately describes the dependence of the lattice spacing on the coupling constant [3] though dimensionless ratios of physical quantities, such as $T_c/\sqrt{\sigma}$ (σ = string tension), are already scaling at the g^2 -values under consideration.

To assess the influence of finite size effects and the numerical and physical problems involved, we show in Fig. 1 previous results for $\langle \bar{L} \rangle$ obtained on $18^3 \times 3$, 4 and 5 lattices [4], i.e. for fixed N_σ and varying N_τ , plotted as a function of T , where T was obtained via (5, 6). We observe, that for increasing N_τ the curves become flatter and only in the very neighbourhood of the transition point we have nearly overlapping functions. This N_τ -dependent behaviour is already known from the weak coupling expansion of $\langle \bar{L} \rangle$ [5] and has two consequences: $\langle \bar{L} \rangle$ is not directly a physical quantity as suggested by (4), because then also for different N_τ we should have one scaling function $\langle \bar{L} \rangle(T)$, and secondly it makes the determination of T_c more difficult for larger N_τ due to the smaller slope of $\langle \bar{L} \rangle$ near T_c . The corresponding plot for fixed N_τ and varying N_σ is schematically drawn in Fig. 2 (see also Fig. 1 of [4]). Here the curves become flatter with decreasing N_σ , they indicate smaller critical temperatures for smaller N_σ ; as expected the determination of the critical point becomes easier with increasing N_σ .

An important point not visible in Figs. 1 and 2 is that even with high statistics in the neighbourhood of the transition the measured points have so large errors,

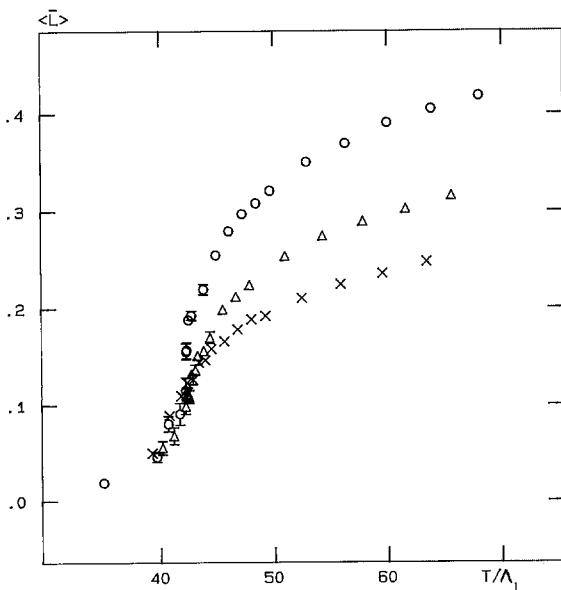


Fig. 1. Order parameter $\langle \bar{L} \rangle$ on $18^3 \times 3$ (O), 4 (Δ) and 5 (\times) lattices vs. T/Λ_L from [4]

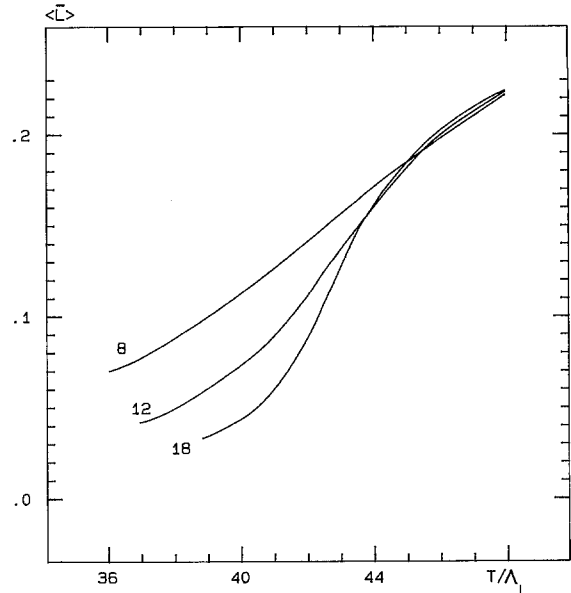


Fig. 2. Schematic plot of $\langle \bar{L} \rangle$ vs. T/Λ_L for $N_\tau = 4$ and $N_\sigma = 8, 12$ and 18

that it is unclear, whether one is above or below the transition and how many iterations are necessary to decide that question. This uncertainty is, of course, related to the increase of the correlation length, when the second order transition point is approached.

In this paper we want to tackle the mentioned problems by studying the distribution functions $P(L)$ for various $4/g^2$. The change of the distributions when the critical point is approached is investigated in Sect. 2 on a $16^3 \times 3$ lattice. In the following section we compare the distributions at one $4/g^2$ -value close to the transition on 8^3 , 12^3 and $18^3 \times 4$ lattices to see explicitly the finite size effects. Section 4 is devoted to the problem of finding a more scaling quantity as order parameter, from which then the critical exponent β may be determined by a direct fit. For this purpose we take our new results and combine them with re-evaluated results from [4]. Our findings are summarized in the last section.

2 The Polyakov loop distribution function

The idea to study the Polyakov loop distribution function was first applied to the Ising model by Binder [6] and later extended to $SU(2)$ by Mitrjushkin and Zadorozhny [7]. The latter authors calculated the distributions for several couplings with a statistics of 7,000 to 8,000 iterations on an $8^3 \times 4$ lattice. We found that this is by far not enough to get reliable results, even on such a small lattice. In general we therefore performed 100,000 sweeps on a $16^3 \times 3$ lattice with a full group heatbath vector programme, which took $5.6 \mu\text{sec}$ per link update. For thermalization no data were measured during the first 1,000 iterations.

The distribution function, which is formally defined

as

$$P(L) = Z^{-1} \int \prod_x dU e^{-S} \delta\left(L - \frac{1}{N_\sigma} \sum_x L(\mathbf{x})\right), \quad (7)$$

is the probability density to find the Polyakov loop value in the interval $[L, L + dL]$. In practice we approximately determined it by measuring the frequency distribution of the lattice average L . The bin size ΔL was chosen such as to have 200 bins between the minimal and maximal L or \bar{L} for a fixed $4/g^2$. Once $P(L)$ is known, expectation values of all powers of L may be calculated from

$$\langle L^\alpha \rangle = \int dL L^\alpha P(L). \quad (8)$$

For comparison we show in Fig. 3 three characteristic distributions $P(L)$ on a $16^3 \times 3$ lattice: below the critical temperature at $4/g^2 = 2.165$, close to, but above T_c at $4/g^2 = 2.18$, and well above T_c at $4/g^2 = 2.20$. Obviously, the curve at the highest temperature is close to a Gaussian, which only on the small \bar{L} side is slightly changed due to some attempts of the system to flip into the other state. Looking at the sweep history of this special Monte Carlo run one identifies one successful phase flip, one nearly successful and several smaller phase flip attempts. At first sight the occurrence of flips cannot be read off the sweep history of other observables such as the space-time plaquette P_τ . Also the frequency distribution of P_τ and P_σ , the space-space plaquette, remain Gaussian even very close to the deconfinement transition. A closer look, such as in Fig. 4, where we show the part of the sweep history of L and P_τ in the neighbourhood of the phase flip at $4/g^2 = 2.20$, reveals, however, that if \bar{L} decreases P_τ becomes slightly larger. This is confirmed by the small negative correlation $\langle (P_\tau - \langle P_\tau \rangle)(L - \langle L \rangle) \rangle$ ($= -0.002$ at $4/g^2 = 2.20$). Approaching the transition

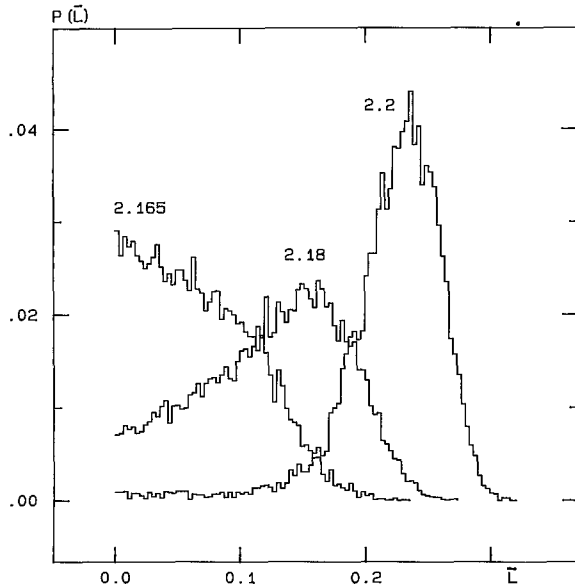


Fig. 3. The distribution $P(\bar{L})$ on a $16^3 \times 3$ lattice for $4/g^2 = 2.165$ (below T_c), 2.18 ($1.02T_c$) and 2.20 ($1.07T_c$)

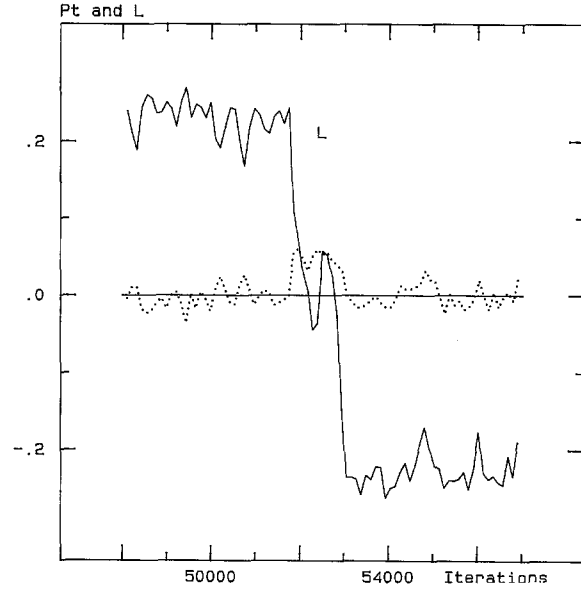


Fig. 4. Sweep history of the Polyakov loop L and $10 \cdot (P_\tau - \langle P_\tau \rangle)$, where P_τ is the space-time plaquette, near a phase flip at $4/g^2 = 2.20$ on a $16^3 \times 3$ lattice. To show the gross structure of the data only averages over 100 iterations are plotted

now from the high temperature side, the number of tunneling attempts will increase and gradually fill the gap between the two states of the system, one at negative, one at positive L . This is seen in Fig. 3 from the curve at $4/g^2 = 2.18$. Very close to the transition it will then be impossible to distinguish the thermal Gaussian from the tunneling effects, since the latter will increase and the width of the Gaussian, being proportional to the susceptibility χ , will reach a maximum. Well below the transition the distribution is expected to become again a Gaussian centered at

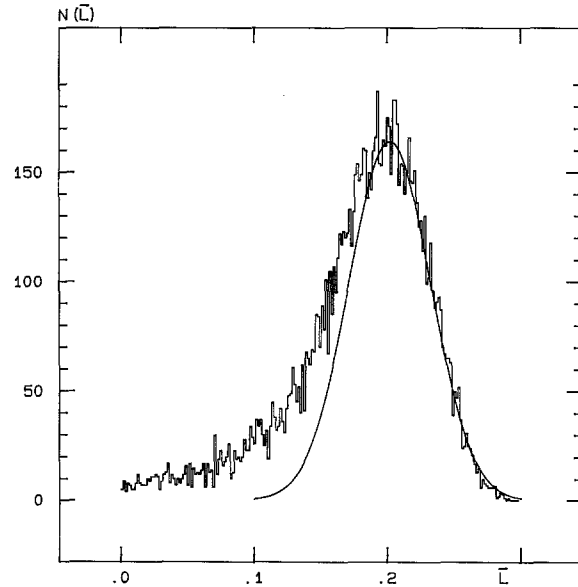


Fig. 5. The frequency distribution $N(\bar{L})$ at $4/g^2 = 2.19$ and a Gaussian fit to its right wing

$L=0$, because only one state exists and there is no tunneling. From the $4/g^2 = 2.165$ distribution in Fig. 3 we see that though the maximum is at $\bar{L}=0$, the function is still different from a Gaussian.

One may now take advantage of this behaviour of the Polyakov loop distribution function to try to separate the tunneling fluctuations from the Gaussian part [7]. For this purpose we fit the large \bar{L} wing of $P(\bar{L})$, which supposedly is undisturbed by tunneling effects by

$$P(\bar{L}) \sim \exp[-(\bar{L} - \bar{L}_{\max})^2 / 2\sigma_L^2], \quad (9)$$

where \bar{L}_{\max} is the peak position of the distribution and σ_L the Gaussian width

$$\sigma_L^2 = \langle \bar{L}^2 \rangle - \bar{L}_{\max}^2. \quad (10)$$

In Fig. 5 we show an example of such a fit at $4/g^2 = 2.19$. The two parameters of the Gaussian fit may then be used for an alternative definition of both the order parameter and the susceptibility, i.e. one may replace $\langle \bar{L} \rangle$ by \bar{L}_{\max} and χ by

$$\chi_G = N_\sigma^3 (\langle \bar{L}^2 \rangle - \bar{L}_{\max}^2) = N_\sigma^3 \sigma_L^2. \quad (11)$$

Both quantities will coincide with their counterparts in the thermodynamic limit. A comparison of the old and new variables is contained in Figs. 6 and 7 and in Table 1. We see, that for $4/g^2$ further away from the critical coupling the two definitions for the order parameter lead to coinciding results, at shorter distances the L_{\max} -values are larger than $\langle \bar{L} \rangle$, so that the derivative of the new order parameter close to the transition becomes much larger. The steeper form of the curve has the consequence that the transition point itself can be easier located and that a corresponding critical exponent fit is more reasonable. For the

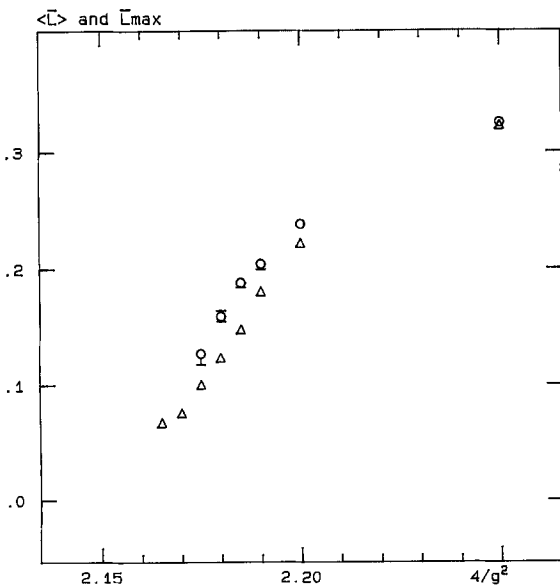


Fig. 6. The order parameter $\langle \bar{L} \rangle$ (Δ) and \bar{L}_{\max} (\circ) on a $16^3 \times 3$ lattice vs. $4/g^2$

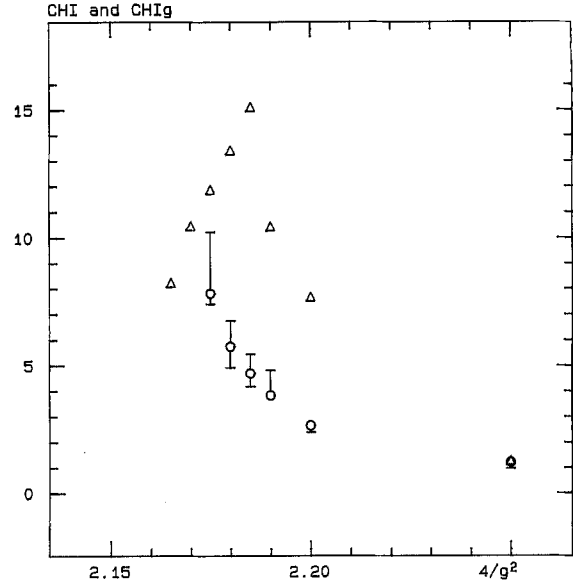


Fig. 7. The susceptibility χ (Δ , errors are large and unknown) and χ_G (\circ) on a $16^3 \times 3$ lattice vs. $4/g^2$

Table 1. Numerical results from the $16^3 \times 3$ lattice

$4/g^2$	Order parameter		
	$\langle \bar{L} \rangle$	\bar{L}_{\max}	$\Delta \bar{L}_{\max}$
2.165	0.0677(18)		
2.170	0.0761(22)		
2.175	0.1006(23)	0.1276	+0.0019 -0.0095
2.180	0.1244(29)	0.1591	+0.0051 -0.0041
2.185	0.1485(38)	0.1877	+0.0031 -0.0040
2.190	0.1806(25)	0.2039	+0.0000 -0.0048
2.200	0.2221(27)	0.2380	+0.0021 -0.0007
2.250	0.3226(04)	0.3246	+0.0023 -0.0003
$4/g^2$	Susceptibility		
	χ	χ_G	$\Delta \chi_G$
2.165	8.24		
2.170	10.46		
2.175	11.88	7.81	+2.42 -0.42
2.180	13.42	5.74	+1.01 -0.83
2.185	15.13	4.69	+0.75 -0.51
2.190	10.45	3.83	+0.98 -0.00
2.200	7.68	2.66	+0.12 -0.26
2.250	1.28	1.21	-0.25

susceptibility it leads to more accurate data points and to a shift of the maximum to lower $4/g^2$ -values, in accord with the results from \bar{L}_{\max} . It is unclear, however, whether the transition point determined by this method is closer to the transition point on the infinite volume lattice.

An often proposed way [8] to reduce the variance of loop expectation values is the one by Parisi et al. [9]. For thermal Wilson loops in $SU(2)$ one would replace all $SU(2)$ link matrices U in (1) by new operators \bar{U} [8], where

$$\bar{U}^{-1} = XI_2(\lambda)/\lambda I_1(\lambda), \quad (12)$$

and

$$UX = \sum_{P(\bar{U})} U_P \quad (13)$$

is the sum of six plaquettes containing a factor U ; the I_1 and I_2 are modified Bessel functions and

$$\lambda = \frac{4}{g^2} (\det X)^{1/2}. \quad (14)$$

We have calculated the distribution function $P(L)$ using the modified links. In Fig. 8 we compare the resulting $P(\bar{L})$ with the one obtained in the usual way for $4/g^2 = 2.297$ on a $12^3 \times 4$ lattice after the same number of sweeps. Of course, the same limiting (i.e. for infinitely many iterations) distribution is expected in both cases. The variance reduction technique does, however, not lead to any visible improvement in the convergence to this distribution. The same is true for correlations of the Polyakov loop.

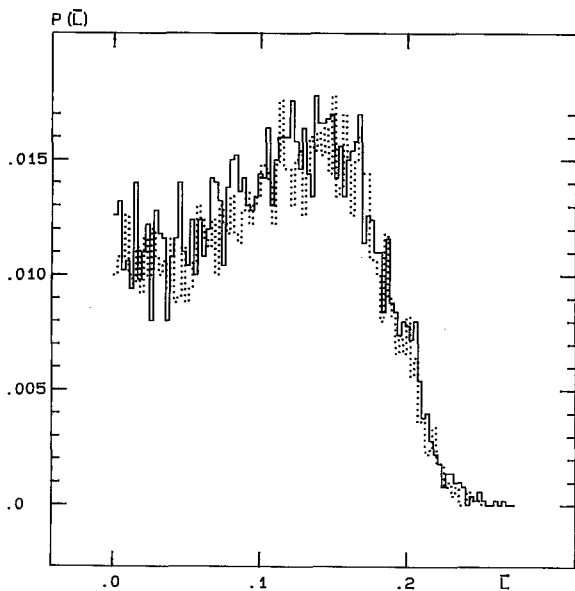


Fig. 8. Comparison of $P(\bar{L})$ obtained with normal (lines) and modified [9] (dots) links on a $12^3 \times 4$ lattice at $4/g^2 = 2.297$ after 50000 iterations each

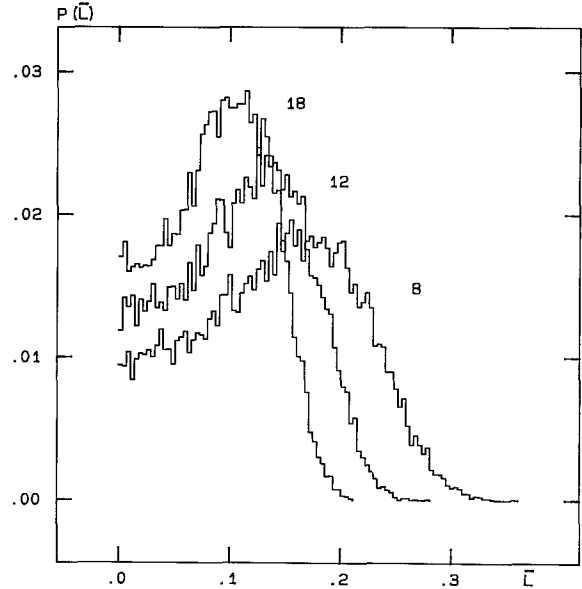


Fig. 9. The Polyakov loop distributions on $8^3 \times 4$, $12^3 \times 4$ and $18^3 \times 4$ lattices at $4/g^2 = 2.297$ (corresponds to $T = 1.02T_c$ on the $N_\sigma = 18$ lattice)

3 Finite volume effects

To see the influence of finite volume effects on the Polyakov loop distributions we compare in Fig. 9 $P(\bar{L})$ as obtained on $8^3 \times 4$, $12^3 \times 4$ and $18^3 \times 4$ lattices after 200,000 sweeps at $4/g^2 = 2.297$. This coupling corresponds to about $1.02T_c$ on the $N_\sigma = 18$ lattice. We observe strong finite size effects. As expected, the width σ_L and the tunneling effects increase with decreasing N_σ , but also \bar{L}_{\max} changes by a factor of two between the $N_\sigma = 8$ and 18 lattices. A smaller critical temperature is therefore to be expected for

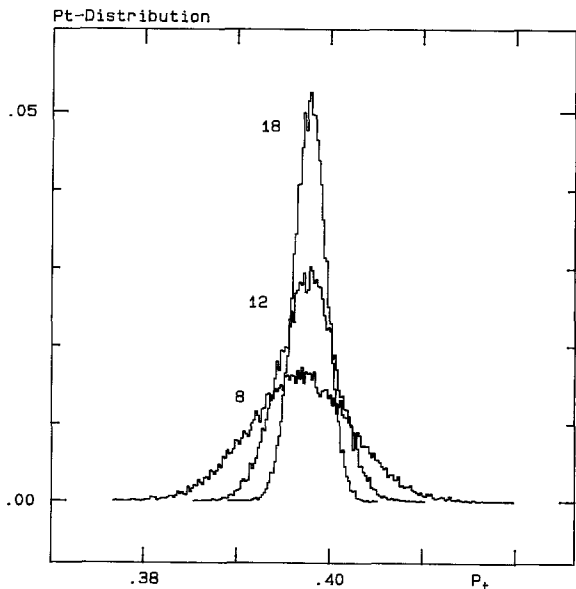


Fig. 10. The space-time plaquette distributions on the same lattices and at the same $4/g^2$ as in Fig. 9

smaller lattices. If one looks at the corresponding space-space and space-time plaquette distributions—the latter are shown in Fig. 10—one finds that they are all Gaussians; despite the close neighbourhood to the transition point no tunneling influence is seen. Of course, the widths of these Gaussians are increasing with decreasing N_σ and, in accord with the weak coupling expansions [5] of the plaquette expectation values, the average values are slightly different. To obtain equally-well-determined distributions for L and/or $P_{\sigma,\tau}$ on these three lattices about the same large numbers of iterations were needed, i.e. essentially no critical slowing down was observed.

4 A physical order parameter

As we have seen in section one, the order parameter $\langle \bar{L} \rangle$ is not directly a physical quantity, but strongly N_τ -dependent. To take away the main N_τ -dependence we therefore propose to use as an order parameter the quantity

$$L_{\text{phys}} = \bar{L}_{\text{max}}/L_{\text{wc}}, \quad (15)$$

where L_{wc} is given by the weak coupling expansion

$$L_{\text{wc}} = 1 - c_1 g^2 - c_2 g^4 + O(g^6), \quad (16)$$

and c_1 and c_2 are known coefficients [5]; c_1 is proportional to N_τ and positive. It is clear then, that the use of the truncated expansion at finite g^2 and large N_τ will lead to negative values of L_{wc} . This approximation may therefore not be used for large N_τ , but for $N_\tau = 3, 4$ and 5 it seems reasonable. For larger N_τ an alternative to L_{wc} is an exponentiated form, inspired by (4),

$$L'_{\text{wc}} = \exp \{ -N_\tau (f_1 g^2 + f_2 g^4 + O(g^6)) \}, \quad (17)$$

where f_1 and f_2 are determined such, that L_{wc} and L'_{wc} coincide up to order $O(g^4)$. The major advantages of L'_{wc} are that it is always positive and that the main N_τ -dependence is explicitly given, since f_1 is independent of N_τ and f_2 only weakly dependent on it. Yet, the corresponding L'_{phys} calculated from our $N_\tau = 3, 4$ and 5 data still show a qualitative behaviour like $\langle \bar{L} \rangle$; therefore we use the direct weak coupling expansion in the following.

We have re-evaluated the $18^3 \times 3, 4$ and 5 data from [4] to obtain \bar{L}_{max} . It was not possible to determine \bar{L}_{max} at all $4/g^2$ -values, because (especially in the very near neighbourhood of T_c) some distributions had in spite of 20–60,000 sweeps too low statistics to allow for a reasonable Gaussian fit. We completed therefore the $N_\tau = 3$ data by including our new $16^3 \times 3$ points, the $N_\tau = 4$ data by new results on $18^3 \times 4$ lattices [10]. The resulting L_{phys} is plotted as a function of the asymptotic T/Λ_L , i.e. using (5, 6) in Fig. 11. Obviously there is still not one scaling function $L_{\text{phys}}(T)$. Most probably this is due to the non-asymptotic $a(g^2)$. As a consequence one cannot determine the critical exponent with high precision by a direct fit to these curves and they cannot be expected to fall on top of each other. However, we can make a virtue of necessity and find the functional behaviour of $a(g^2)$ by demanding that L_{phys} must have the same temperature regardless of N_τ . Comparing two curves with different N_τ one has for two equal L_{phys} the temperature

$$T^{(1)} = \frac{1}{N_{\tau 1} a(g_1^2)} = \frac{1}{N_{\tau 2} a(g_2^2)}. \quad (18)$$

Suppose $a(g^2)$ is known at one of the points, say $a(g_1^2)$,

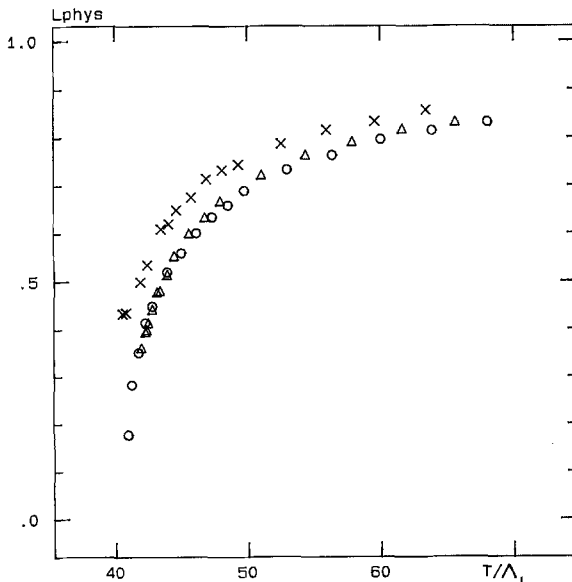


Fig. 11. The order parameter L_{phys} vs. the asymptotic temperature for $18^3 \times 3$ (\circ), 4 (\triangle) and 5 (\times) lattices

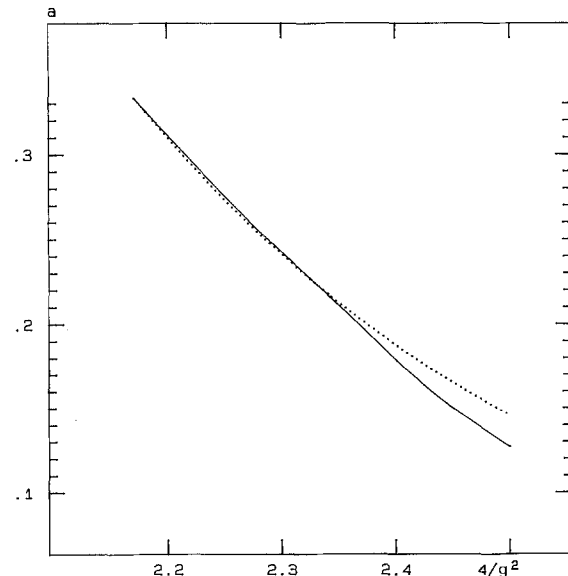


Fig. 12. The lattice spacings $a(g^2)$, non-asymptotic (line) and asymptotic (dotted) vs. $4/g^2$

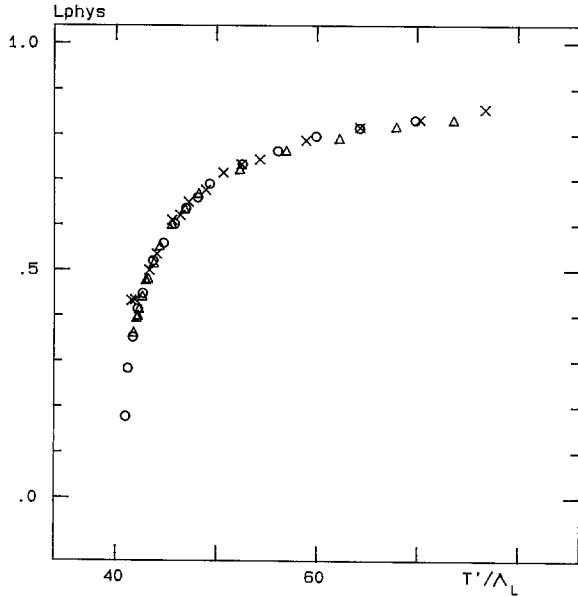


Fig. 13. The order parameter L_{phys} vs. the temperature T' , which was calculated from the non-asymptotic $a(g^2)$; T' was normalized to the asymptotic temperature at $4/g^2 = 2.171$. The notation is like in Fig. 11

then

$$a(g_2^2) = \frac{N_{\tau 1}}{N_{\tau 2}} a(g_1^2). \quad (19)$$

If the g^2 -regions of the two N_{τ} -curves overlap, it is possible to proceed, since one may make a new comparison at

$$T^{(2)} = \frac{1}{N_{\tau 1} a(g_2^2)} = \frac{1}{N_{\tau 2} a(g_3^2)} \quad (20)$$

and so forth. Finally, one has a set of g^2 -values, where $a(g^2)$ is known in terms of $a(g_1^2)$, which sets the scale. Of course, two curves may always be superimposed in this way, but it is non-trivial when a third curve coincides with the first two. In Fig. 12 we show the new function $a(g^2)$ obtained with the described method and the asymptotic form from (6) both in units of $T_c(N_{\tau} = 3)$, i.e. at $4/g^2 = 2.171$ the plots were normalized to $1/3$. The functions differ only slightly ($\leq 1\%$) below $4/g^2 = 2.35$, up to $4/g^2 = 2.5$ the difference is increasing to about 15% . The somewhat steeper slope of the new $a(g^2)$ is in full accord with the $\Delta 4/g^2$ -values (at $4/g^2 = 2.5$ we have $\Delta 4/g^2 \approx 0.225$) found via MCRG methods [3]. With the new scale for the temperature induced by the change in $a(g^2)$ the new order parameter $L_{\text{phys}}(T')$ is then one scaling function for $N_{\tau} = 3, 4$ and 5 as can be seen in Fig. 13. Including all the points in a critical exponent fit of the form

$$L_{\text{phys}} = A(T' - T_c)^\beta (1 + B(T' - T_c)^{0.5}), \quad (21)$$

we find $\beta = 0.324$. With the 95% confidence level method the error is 0.025. The universality hypothesis [11] expects the critical exponents of the (3 + 1)-

dimensional $SU(2)$ gauge theory to coincide with the corresponding exponents of the 3-dimensional Ising model, where β is estimated to be 0.3265 ± 0.0025 [12]. Our result is therefore in excellent agreement with the universality hypothesis.

5 Summary

We have demonstrated the use of Polyakov loop distributions. In the close neighbourhood of the deconfinement transition reliable estimates of the average of the order parameter and the susceptibility will only be obtained if the distributions are well determined, which may require 100,000 to 200,000 sweeps.

The distributions contain a thermal Gaussian part plus additional contributions which are due to tunneling attempts of the system. Even rather close to the transition these parts may be separated by corresponding fits; the location of the maximum and the width of the Gaussian may serve as new order parameter and susceptibility [7] and allow for better critical exponent fits.

Polyakov loop values which are obtained with the Parisi, Petronzio and Rapuano method [9] do not lead to improved distributions.

There are strong finite volume effects in the Polyakov loop and plaquette distributions. Critical slowing down was, however, not observed for the calculation of the distributions, to obtain smooth distributions about the same large number of iterations were necessary on all used lattices.

The quantity L_{phys} may serve as new physical order parameter. It is possible to rescale $a(g^2)$ such that for $N_{\tau} = 3, 4$ and 5 all curves have the same temperature dependence. The non-asymptotic $a(g^2)$ is well in accord with MCRG studies [3]; the critical exponent fit to the scaling L_{phys} leads to a value $\beta = 0.324$ strongly supporting the universality hypothesis [11].

Acknowledgements. It is a pleasure to thank H. Satz and F. Karsch for many helpful discussions, in particular on questions related to the scaling of the order parameter. We are indebted to the Bochum University computer centre for providing the necessary Cyber 205 time.

References

1. K. Wilson: Phys. Rev. D10 (1974) 2445
2. L. McLerran, B. Svetitsky: Phys. Lett. 98B (1981) 195; Phys. Rev. D24 (1981) 450; J. Kuti, J. Polónyi, K. Szalchányi: Phys. Lett. 98B (1981) 199
3. U. Heller, F. Karsch: Phys. Rev. Lett. 54 (1985) 1765
4. J. Engels, et al.: Nucl. Phys. B280 [FS18] (1987) 577
5. U. Heller, F. Karsch: Nucl. Phys. B251 [FS13] (1985) 254
6. K. Binder: Z. Phys. B-Condensed Matter 43 (1981) 119
7. V.K. Mitrjushkin, A.M. Zadorozhny: Phys. Lett. 185B (1987) 377
8. F. Karsch, C.B. Lang: Phys. Lett. 185B (1984) 176
9. G. Parisi, R. Petronzio, F. Rapuano: Phys. Lett. 128B (1983) 418
10. J. Engels, J. Fingberg, M. Weber: Bielefeld Preprint (1988), in preparation
11. B. Svetitsky, L.G. Yaffe: Nucl. Phys. B210 [FS6] (1982) 423
12. J.C. Le Guillou, J. Zinn-Justin: J. Phys. Lett. 46 (1985) L137